



# Predicting growth plate orientation with altered hip loading: potential cause of cam morphology

S. Mahsa Sadeghian<sup>1</sup> · Cara L. Lewis<sup>3</sup> · Sandra J. Shefelbine<sup>1,2</sup>

Received: 24 April 2019 / Accepted: 14 October 2019 / Published online: 11 November 2019  
© Springer-Verlag GmbH Germany, part of Springer Nature 2019

## Abstract

Proximal femoral deformities can result from altered hip joint loading patterns during growth. The growth plate hyaline cartilage has low resistance to shear stress. Therefore, we hypothesized that the growth plate orients in a direction which minimizes the shear stress on its surface. A finite element model of the proximal femur was generated with a simplified flat growth plate. Hip joint forces were estimated for standing upright and standing in hip flexion. We also parametrically studied the effects of posteriorly and laterally directed loads. An algorithm was developed to predict the shape of the femoral growth plate in a plane of minimum shear (along the principal stress vectors). To characterize and compare the growth plate shapes, we represented the distance from the growth plate to a reference plane as a two-dimensional contour plot, providing information of shape and orientation across the entire surface. We also assessed the clinical measures of growth plate shape to compare our predicted growth plates with previous clinical studies data. The shape of the growth plate predicted for an upright standing load correlated closely with morphological properties of the growth plate of a typically developing child. The shape of the growth plate predicted for femoral hip flexion force was similar to the growth plate in subjects with cam morphology, a hip shape that has documented growth plate changes. The model proposed here allows for investigation of the relation between joint forces and growth plate shape, which will help predict the development of bony deformities.

**Keywords** Musculoskeletal · Finite element analysis · Biomechanics · Bone deformity development · Femoral growth plate

## 1 Introduction

Longitudinal bone growth takes place in a thin layer (2–5 mm) of hyaline cartilage, called the growth plate or epiphyseal plate. This cartilaginous plate, which is located between epiphysis and diaphysis of the long bones, forms bone via endochondral ossification, a process that consists of proliferation, hypertrophy, apoptosis and mineralization of the chondrocytes. Several factors such as genetics, hormones, nutrition and mechanical stresses regulate the rate and location of this process (Villemure and Stokes 2009).

Bone deformities change the range of motion and gait mechanics (Carriero et al. 2014; Lewis et al. 2018a). Moreover, gait alterations change the stress distribution and growth pattern in the bones (Carter and Wong 1988a). Better understanding of the mechanism of the developmental abnormalities and early intervention in children while their growth plates are still open can be a key factor in prevention of bone deformities and subsequent health problems such as early osteoarthritis (Ganz et al. 2003). We looked at the relation between stress distribution and growth pattern with a focus on the proximal femur morphology.

The growth plate of the femur's proximal head critically influences the functionality and range of motion in the hip joint (Shapiro 2002) despite being responsible for only 30% of the length growth in the femur. The proximal femur is particularly prone to growth disturbances, resulting in altered bone morphology, which is likely mechanically driven by hip joint forces and muscle loads during different activities. For instance, loads experienced in utero result in developmental dysplasia of the hip and increased neck-shaft angle (Carriero et al. 2011; Giorgi et al. 2015); loads from cerebral

✉ Sandra J. Shefelbine  
s.shefelbine@northeastern.edu

<sup>1</sup> Department of Mechanical and Industrial Engineering, Northeastern University, Boston, MA, USA

<sup>2</sup> Department of Bioengineering, Northeastern University, Boston, MA, USA

<sup>3</sup> Department of Physical Therapy & Athletic Training, College of Health and Rehabilitation Sciences: Sargent College, Boston University, Boston, MA, USA

palsy gait influence femoral anteversion and neck-shaft angle (Shefelbine and Carter 2004a); adolescent obesity is a primary risk factor for slipped capital femoral epiphysis (SCFE) (Poussa et al. 2003); and specific sports participation during growth increases the risk of cam morphology associated with femoroacetabular impingement (FAI) syndrome (Johnson et al. 2012; Sankar et al. 2013; Siebenrock et al. 2011, 2013a, b).

Despite the recent debates on the reliability of clinical parameters obtained from single slice MRI images (Atkins et al. 2019; Barton et al. 2011; Clohisy et al. 2009), they are still widely used in medical clinics. Clinically, the morphology of the femoral growth plate has been described by epiphyseal angle, epiphyseal tilt and epiphyseal extension (Fig. 1) (Novais et al. 2018). Epiphyseal angle is the angle between the neck axis and a line that connects the head center to the superior side of the growth plate. Epiphyseal tilt is the angle between a line perpendicular to the neck axis and a line that connects two ends of the growth plate. The relative epiphyseal extension (EE) is the distance between each end of the growth plate and a line perpendicular to the neck axis and tangent to the head, divided by the diameter of the femoral head (Siebenrock et al. 2004).

The epiphyseal angle decreases with age, but there is no consistent report on epiphyseal tilt in different age groups (Monazzam et al. 2013; Novais et al. 2018). Epiphyseal extension increases significantly over the years that the growth plate is still open as it assumes a more convex shape during growth (Kienle et al. 2012). Statistical studies on the three-dimensional shape of the proximal end of the femur in patients with cam morphology and FAI syndrome indicated excessive bone on the anterosuperior region of head-neck junction (Harris et al. 2013a, b; Kang et al. 2013). In femurs with cam morphology, epiphyseal tilt is smaller than the normal range (Monazzam et al. 2013) and anterior epiphyseal extension is greater in the anterosuperior plane compared to femurs without cam (Siebenrock et al. 2004). In particular, there is a significant increase in epiphyseal extension and prevalence of anterior–superior cam deformity (deemed as alpha angle

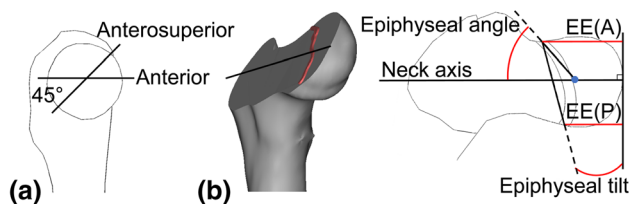


**Fig. 1** Proximal femur clinical parameters. **a** Radially oriented planes around the neck axis. **b** The anatomical measurements in the anterosuperior plane, epiphyseal angle, epiphyseal tilt, epiphyseal extension on the anterior side (EE (A)) and epiphyseal extension on the posterior side (EE (P))

greater than 55°) in children with open growth plates who participate in ice hockey, soccer and basketball practices (Agricola et al. 2014; Siebenrock et al. 2011, 2013a, b). These studies illustrated the importance of mechanical loads as the main factor in the development of cam morphology. However, there is little understanding of how altered loading causes bone deformities.

Using the fact that altered joint forces influence growth and total bone shape finite element models of the proximal femur have shown that the shape and orientation of the growth plate significantly affects the stresses in the growth plate (Carriero et al. 2011; Shefelbine and Carter 2004a, b; Yadav et al. 2016). Computational models have suggested that changes in growth plate morphology during growth reduce octahedral shear stress within the growth plate (Castro-Abril et al. 2016). It has also been shown that an increased neck-shaft angle is due to different growth rates across the growth plate (the medial side growing faster than the lateral side), and an increased anteversion is due to changes in the direction of growth (resulting in twisting during growth) (Shefelbine and Carter 2004a, b). Some morphological and structural alterations of the growth plate decrease the stability of the growth plate, making it more prone to slippage and increasing the risk of SCFE, even within the physiological stress range (Farzaneh et al. 2015; Gómez-Benito et al. 2007). Previous studies have indicated the importance of growth plate shape on total growth behavior and bone morphology. However, the relationship between the primary loading direction and the orientation of the growth plate is unclear.

It has been proposed that the stress distribution in the growth plate affects growth and ossification. In particular, hydrostatic pressure maintains cartilage and shear stress promotes ossification (Carter and Wong 2003). In addition, the growth plate cartilage has low shear strength and shear stress at the proximal growth plate reduces hip joint stability. Both these factors (high shear stress and instability) lead to joint degeneration (Chung et al. 1976; Clohisy et al. 2009; Kandzierski et al. 2012; Smith 1962; Zupanc et al. 2008). Therefore, we hypothesize that the growth plate orients in a direction which minimizes the shear stress on its surface. We simulated growth plate shape and orientation in order to minimize the average shear stress on the proximal side of the growth plate (since it has been shown that the direction of the cell column in the proliferative zone is determined in the resting zone and these columns direct the growth (Abad et al. 2002)). We examined specific loading conditions and compared the predicted growth plates with published clinical measures and MR images. This model could provide an explanation for bone deformities that arise in different conditions as well as a guide for appropriate loading on the bone to maintain growth plate shape.

## 2 Methods

### 2.1 Finite element analysis

#### 2.1.1 Mesh and material

Initially, a finite element model of the proximal femur of a 7-year-old subject was generated, including a generic “flat” growth plate (Yadav et al. 2016). The growth plate and transition zone (6 mm right below and above the growth plate) were meshed with quadratic tetrahedron elements, while the distal areas (greater trochanter, shaft and distal end of the bone) had linear tetrahedron elements. This might cause noncompatible displacement field far away from our region of interest which would not affect our results. In total, twenty-five models were solved and each model consisted of approximately 575,500 nodes and 435,000 elements with the average element size of 1.28 mm (minimum element size of 0.8 mm in the growth plate and maximum 1.7 mm in the distal end) and a mesh convergence study proved the mesh independency of the results (ABAQUS version 6.13-2, Simulia, Providence, RI, USA).

Despite the poroelastic nature of the cartilage, a linear elastic, homogeneous and isotropic model was used to represent its properties under quasi-static loads, since low permeability of the cartilage allows fluid flow during short periods of loading (Carter and Wong 2003). The Young’s Modulus for growth plate, trabecular bone and cortical bone were assigned as 5 MPa, 600 MPa and 20GPa (Carriero et al. 2011), respectively. In the transition zone, this modulus linearly varied from 5 MPa to 600 MPa with distance from growth plate (Carriero et al. 2011; Yadav et al. 2016, 2017). The transition zone on the metaphyseal side represents a gradient (Radhakrishnan et al. 2004) in mineralization beneath the growth plate as full mineralization occurs over long time scale. It also prevents an abrupt change in the material properties between cartilage and adjacent bones. We found that the results were not sensitive to the gradient of the transition zone on the epiphyseal side but were sensitive to the gradient of the transition zone on the metaphyseal side. The Poisson’s ratio of cartilage was considered as 0.48 (nearly incompressible) and 0.3 for all other regions (Fig. 2).

#### 2.1.2 Loading and boundary condition

The distal end of the femur was fixed in all directions to prevent the model from rigid translation. Also, ten nodes on the greater trochanter were fully constrained to simulate the hip abductor muscle group (Fig. 3a). The resultant hip

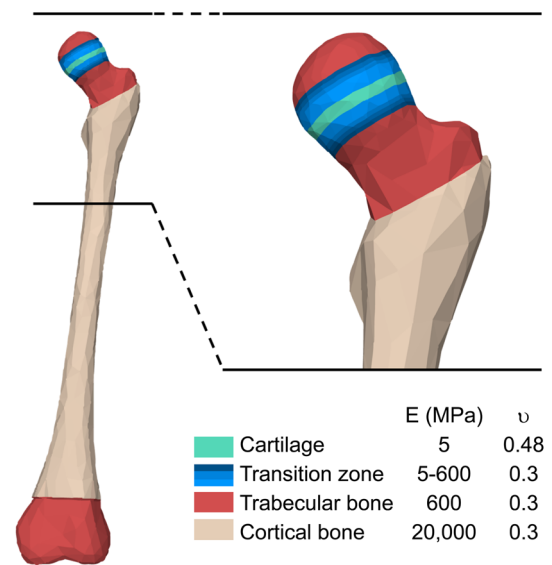


Fig. 2 Femur geometry and material properties

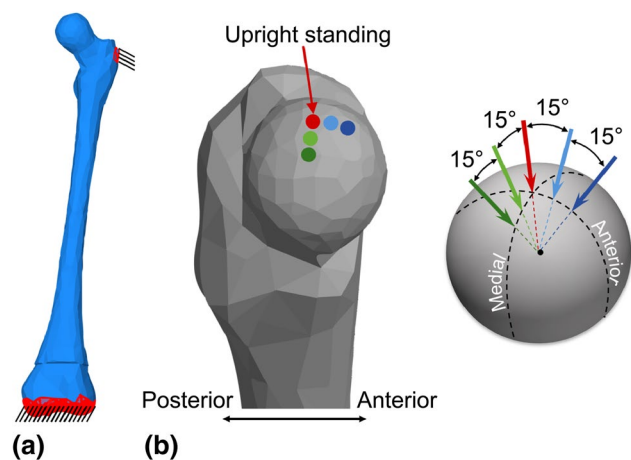


Fig. 3 Loading and boundary conditions. **a** The distal end of the femur and 10 nodes on the greater trochanter were fully constrained. **b** Resultant hip joint forces were measured for upright standing. Four parametric loads were defined in sagittal and frontal planes directed laterally and posteriorly, respectively

joint contact force used in this study included the effect of muscle forces on the joint force; however, the muscle forces were not considered separately in this study since their direct impact on local principal stress distribution direction in the growth area was shown to be negligible in comparison to joint force (Yadav et al. 2017). A sensitivity study showed that these simplifications do not affect the final results significantly since all the muscle attachments are below the growth plate.

Resultant hip joint forces were measured standing upright and standing with hip flexion in a gait laboratory. While

the upright standing load represented an average load for a typically developing child, the hip flexion load was considered as an average load that children experience during ice hockey practices, a group with high prevalence of anterior–superior cam morphology (Agricola et al. 2014; Siebenrock et al. 2011, 2013a; b). In addition, previous studies have shown that subjects with FAI syndrome, indicating the presence of characteristic morphology, signs and symptoms, move with increased hip flexion and anterior pelvic tilt (Lewis et al. 2018a, b). Here, we explore if increased hip flexion may be the cause of cam morphology rather than the result of the morphology. In order to systematically explore the relation between the load shift and growth plate tilt, four parametric loads were defined with 15 and 30 degree tilt in the sagittal and frontal planes directed laterally and posteriorly, respectively (Fig. 3b; Table 1). The directions were chosen based on the range of hip joint force directions in routine activities such as walking, running, going up and down the stairs, standing up and sitting down and standing on one leg (Bergmann et al. 1993, 2001, 2016). The magnitude of the collected data was scaled with respect to the average body weight of 7-year-old children (22 kg) and it is constant through all the simulations. All the loads were centered at the center of the femoral head (hip joint center) and uniformly spread over approximately 5 mm<sup>2</sup> area on the femoral head surface.

### 2.1.3 Growth plate geometry and stress analysis

A custom MATLAB (MathWorks, Massachusetts, USA) algorithm was developed to use the finite element analysis results and predict the orientation of the femoral growth plate by creating a surface along the principal stress directions. A fixed reference point was selected where the neck axis coincided with the growth plate in MRI images. The initial baseline growth plate was flat, 3 mm thick and perpendicular to the neck axis (Fig. 5a). The uniform thickness of the growth plate and transition zones was preserved

**Table 1** Hip contact forces. The coordinate system was defined as: *x*-axis posterior/anterior (+*x* anterior), *y*-axis inferior/superior (+*y* superior) and *z*-axis was defined by cross-product of *x*- and *y*-axes with the origin at the center of the head

	Direction		
	<i>X</i>	<i>Y</i>	<i>Z</i>
Standing upright	0.05	−0.99	−0.04
Standing with hip flexion	−0.58	−0.79	−0.18
15° laterally directed	0.05	−0.95	−0.29
30° laterally directed	0.04	−0.84	−0.53
15° posteriorly directed	−0.21	−0.98	−0.04
30° posteriorly directed	−0.45	−0.89	−0.03

through all the simulations in this study. The simulations iteratively moved the growth plate and the transition zones in the proximal femur to minimize shear stress.

Considering that the shear stress is zero in the direction of principal stress, the plane of minimum shear stress at each point was determined from the principal stresses. Starting at the fixed middle point on the proximal side of the growth plate, a plane perpendicular to the maximum absolute principal stress vectors was defined,

$$a_0x + b_0y + c_0z - (a_0x_0 + b_0y_0 + c_0z_0) = 0 \quad (1)$$

where  $\vec{V} = (a_0, b_0, c_0)$  is the principal stress vector and  $p_0 = (x_0, y_0, z_0)$  is the corresponding point. By moving along the *x*-axis for a specific length (*l*) over this plane,

$$a_0(x_0 + l) + b_0y_0 + c_0z_1 - (a_0x_0 + b_0y_0 + c_0z_0) = 0 \quad (2)$$

The coordinates of the next point was found as  $p_1 = (x_0 + l, y_0, z_1 = z_0 - a_0l/c_0)$  where *l* is the increment length which depends on the elements size of finite element model and in our model was 0.8 mm. Next, a new plane perpendicular to the local maximum absolute principal stress vectors at the new point was defined and the next following point was found. The same process was repeated along the *y*-axis and continued until face increments covered the entire surface (Fig. 4).

In this manner, each face increment is locally perpendicular to the maximum absolute principal stress vectors and the other principal directions were tangent to the face increments. After the region with the minimum shear stress was determined, the model was remeshed and the finite element analysis with new material distribution and same loading condition was performed to evaluate the stress on the proximal side of the growth plate. As the growth plate changed, the surface became more perpendicular to the principal stress vectors (Fig. 5b). Throughout this process, the location of the growth plate changed, moving the material properties and transition zone with it. The element size, boundary and loading conditions remained the same for each iteration. The process was performed iteratively until the shape of the growth plate stabilized and shear stress in the growth plate converged to a minimum (Fig. 5c).

## 2.2 Growth plate characterization

### 2.2.1 Clinical reference parameters

The epiphyseal extension, epiphyseal angle and epiphyseal tilt were measured in anterior and anterosuperior planes for growth plate models of upright standing and parameterized loads. First, a sphere was fitted to the model to find the femoral head center. To determine the neck axis, we filled the neck with the maximum size spheres along the length of the neck; the center of these spheres along with the head

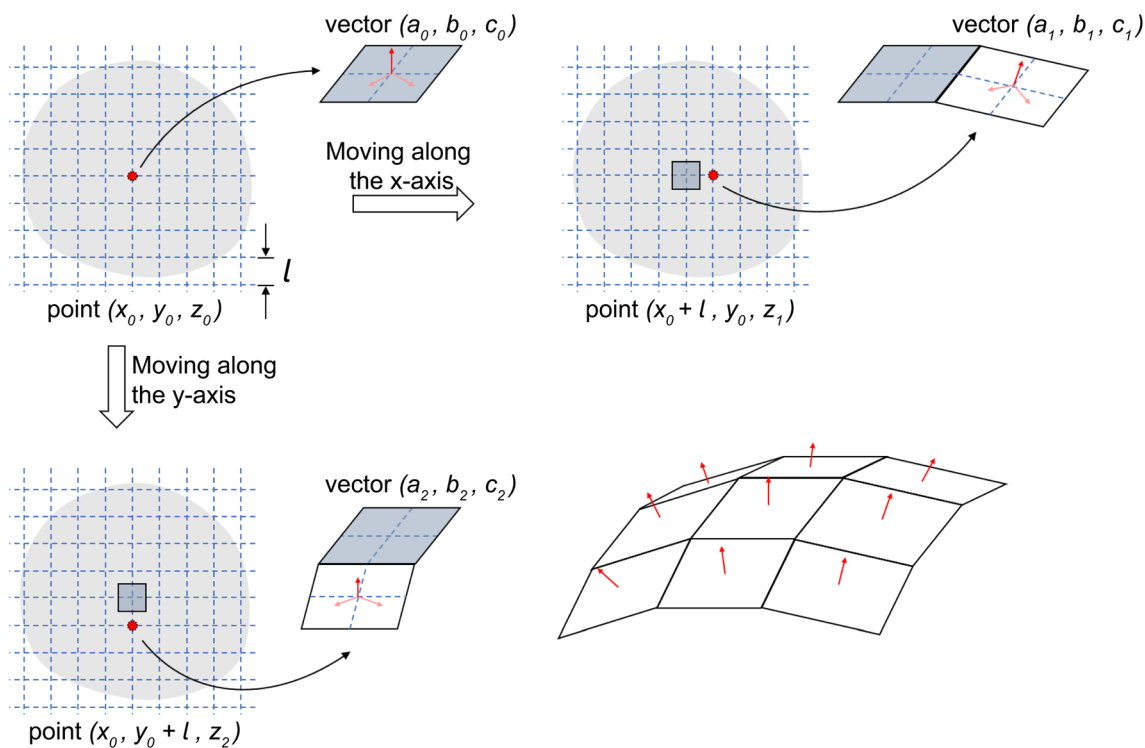
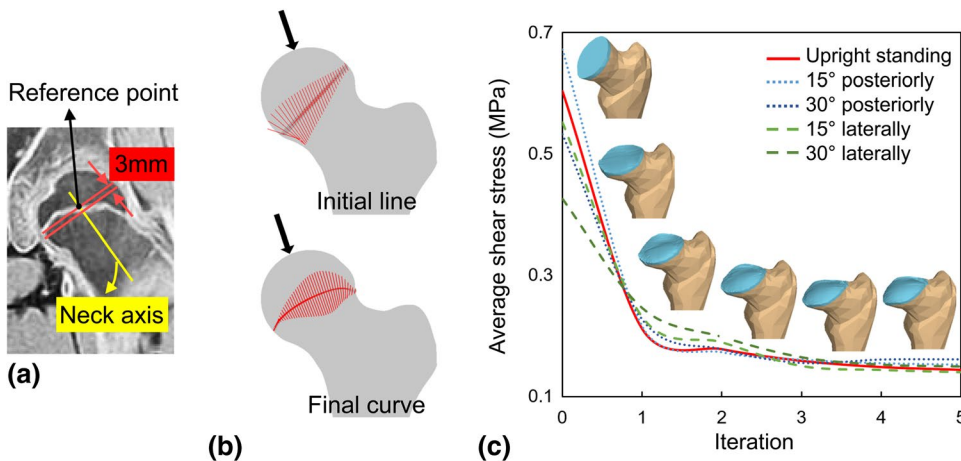


**Fig. 4** Algorithm overview. The growth plate was gridded over the  $xy$ -plane. The  $z$ -coordinate of each point was found using principal stress vectors. At each point, the minimum absolute principal stress vector was used to define a face increment at that point (Eq 1). By

moving along the  $x$ - and  $y$ - axes the whole surface was covered with face increments which were locally perpendicular to the principal stress vector

**Fig. 5 a** The red lines indicate the cutting planes perpendicular to the neck axis. These planes were used to make the baseline growth plate. **b** The final surface is locally perpendicular to principal stress vectors (red lines). **c** Growth plate's geometry changed over iterations and the reduction in average shear stress over the growth plate over the iterations



center was used to determine the neck axis (Fig. 6a). Using the neck axis and center of the femoral head, anterior and anterosuperior planes were defined (Novais et al. 2018).

**2.2.2 Contour**

The efficiency of the two-dimensional measurements in characterizing the morphological properties of the proximal femur has been under debate for many years (Barton

et al. 2011; Clohisy et al. 2009). Although the clinical measurements (epiphyseal tilt, angle, and extension) characterize growth plate orientation and shape in specific planes, they do not portray the 3D orientation of the growth plate relative to the femur. To overcome the limitations of two-dimensional measurements, three-dimensional evaluations had been used previously to assess the difference in proximal femur shape between typically developing and subjects with cam morphology (Audenaert

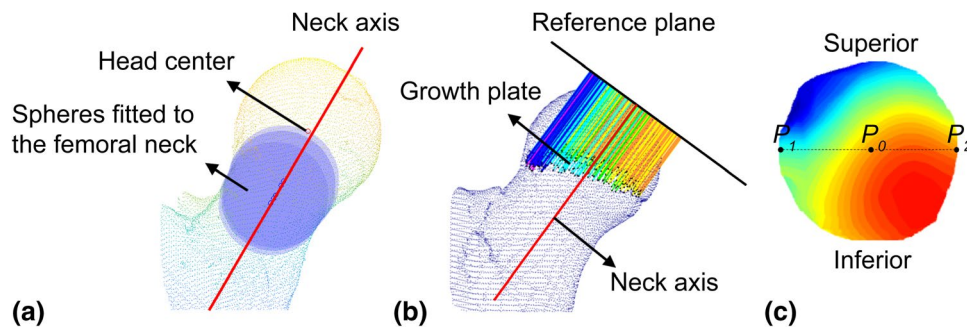


**Fig. 6** Contour plots. **a** Several spheres were fitted into the neck and neck axis was found using the center of the spheres. **b** A plane was defined perpendicular to the neck axis and tangent to the top of the

head. **c** The height of the growth plate with respect to the plane was plotted. Dashed line indicates the anterior–posterior plane cross section and corresponding points are marked

et al. 2011; Harris et al. 2013a, b), but not for the femoral growth plate shape.

We developed a method for comparing the growth plate's 3D morphological features and orientation. A plane perpendicular to the neck axis and tangent to the femoral head was defined and at each point the distance between this plane and the growth plate and was plotted (Fig. 6b). Using this method, the 3D geometries were translated into 2D contour plots as shown in Fig. 6c to assess growth plate orientation.

Every chord of this circular shape represents one cross section of the femoral head. On each chord two endpoints, ( $P_1$  and  $P_2$ ) and the middle point ( $P_0$ ) can be used to evaluate clinical parameters such as epiphyseal extension, epiphyseal angle and epiphyseal tilt as follow,

Epiphyseal extensions at each endpoint are equivalent to the epiphyseal extension at the corresponding cross section.

$$\text{Epiphyseal angle} = \tan^{-1} \left( \frac{h_1 - h_0}{d_{01}} \right) \quad (3)$$

$$\text{Epiphyseal tilt} = \tan^{-1} \left( \frac{h_1 - h_2}{d_{12}} \right) \quad (4)$$

where  $d_{01}$  is the distance between  $P_0$  and  $P_1$ ,  $d_{12}$  is the distance between  $P_1$  and  $P_2$ , and  $h_0, h_1$  and  $h_2$  are the height of the corresponding points.

### 3 Results

Simulated growth plates were found that aligned with the principal stress vectors and minimized the shear stress across the surfaces. Average in-plane shear stress over the epiphyseal side of the growth plate reduced by 80% after five iterations (Fig. 5c). For upright standing load, our simulations predicted a convex growth plate in which the medial side of the growth plate moved closer to the

reference plane and the lateral side moved further away from the reference plane compared to the initial flat growth plate (Fig. 7).

Generally, when loads were in a direction off the vertical axis, the growth plate tilted so the surface of the growth plate oriented perpendicular to the direction of the load. Specifically, when loads were directed laterally, the growth plate tilted medially (anterior-medial side moved inferiorly; posterior-lateral portions moved superiorly) thus perpendicular to the load. The growth plate tilted more medially as the lateral angle increased. With the posteriorly directed load, the growth plate tilted anteriorly, the anterior-lateral portions of the growth plate were below the reference plane while the medial-posterior portions were above the plane (again to be approximately perpendicular to the loading vector). Similarly, as the load tilt angle increased, the growth plate tilted more posteriorly. All predicted growth plates maintained convexity.

The anatomical parameter values for upright standing model were within the normal range of clinically measured growth plates; thus, it was used as a reference to compare the other models. In general, posteriorly directed loads increased the epiphyseal extension on the anterior side and decreased epiphyseal extension on the posterior side. In contrast, laterally directed loads decreased the epiphyseal extension on the anterior side and increased it on the posterior side.

In the anterior plane (Fig. 8a), as the joint force was directed posteriorly by 15 and 30°, the epiphyseal tilt changed from  $-3.7^\circ$  for the standing load to 20 and 28.72° and the epiphyseal angle decreased from 63.4° to 41.4° and 36.5°, respectively. The change in epiphyseal tilt and angle were not notable for the laterally directed loads.

On the anterosuperior plane (Fig. 8b), as the joint force was directed more laterally by 15° and 30° the epiphyseal tilt changed from 14.7° for the standing load to 4.7° and  $-4.9^\circ$  and the epiphyseal angle increased from 47.7° to 55.7° and 62.55°, respectively. No notable change in those parameters was found under the posteriorly directed

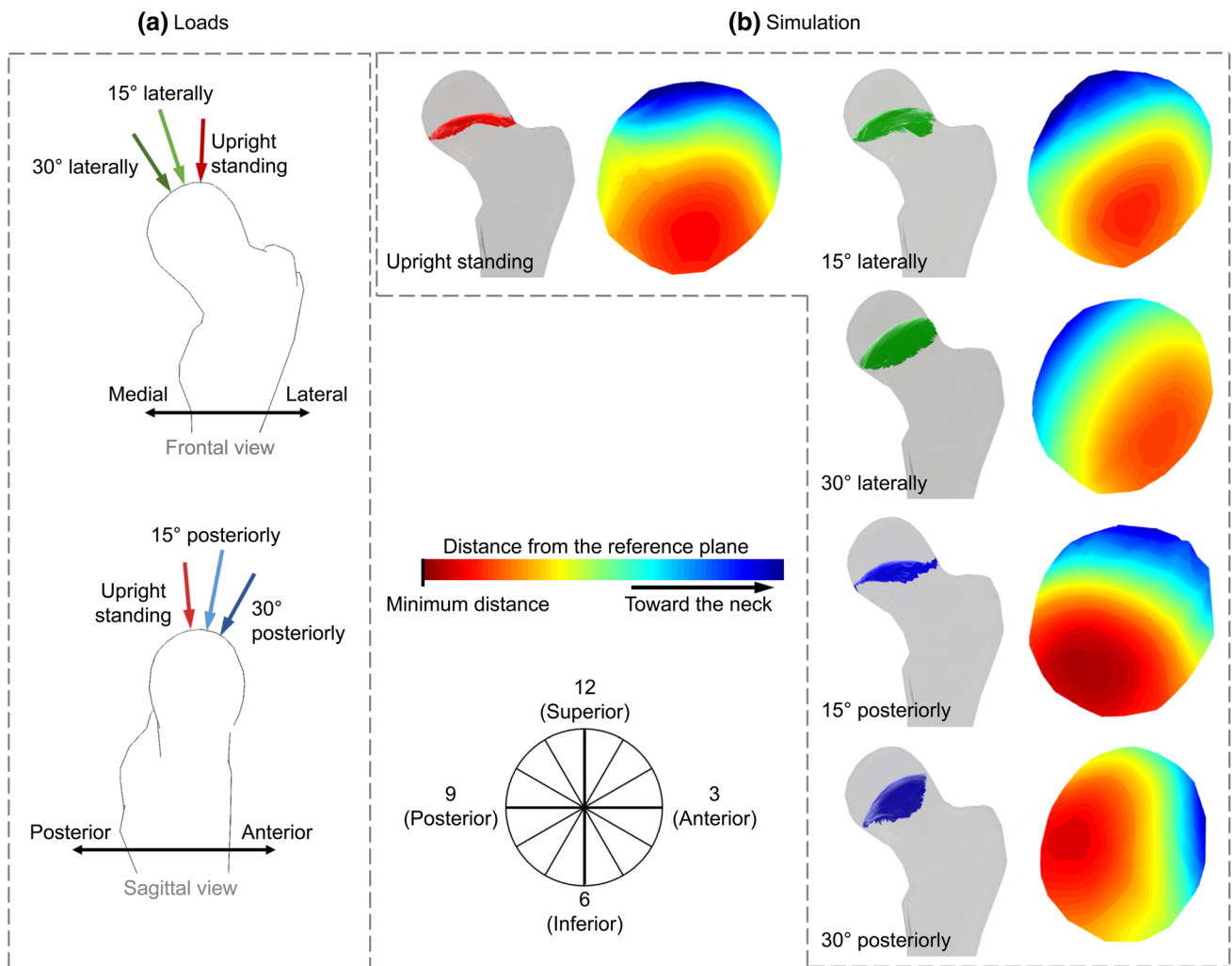


**Fig. 7** Simulated growth plates for upright standing and parametric loads. **a** The locations of the hip joint forces for standing, posteriorly and laterally directed loads. **b** Frontal view of the simulated femo-

ral growth plates and height of the growth plates with respect to the defined reference plane for upright standing and parametric loads (Fig. 3b) are indicated

loads. On this plane, the change in epiphyseal tilt and angle were minimal for the posteriorly directed loads.

To compare the predicted growth plate with clinical data, 2D contours were found from MR images (Palmer et al. 2018) of typically developing subjects and subjects with cam morphology (Fig. 9). The predicted growth plate for the hip flexion load was similar to the growth plate for cam morphology. For both cases the anterosuperior part (between 12 and 3 o’clock) of the growth plate moved further from the reference plane in comparison to standing and typically developing cases. This is the portion of the growth plate to demonstrate measurable differences in children with femoroacetabular impingement.

### 4 Discussion

The hip joint force influences proximal femoral morphology during growth. Many conditions such as obesity, specific athletic activities and cerebral palsy change the joint force and in early ages can result in bone deformities (Agricola et al. 2014; Poussa et al. 2003; Siebenrock et al. 2011, 2013a, b). Slipped capital femoral epiphysis and cam morphology are examples of abnormal bone growth effected by altered stress patterns. In this study, we predicted the growth plate orientation to minimize shear stress under different loading conditions. We examined

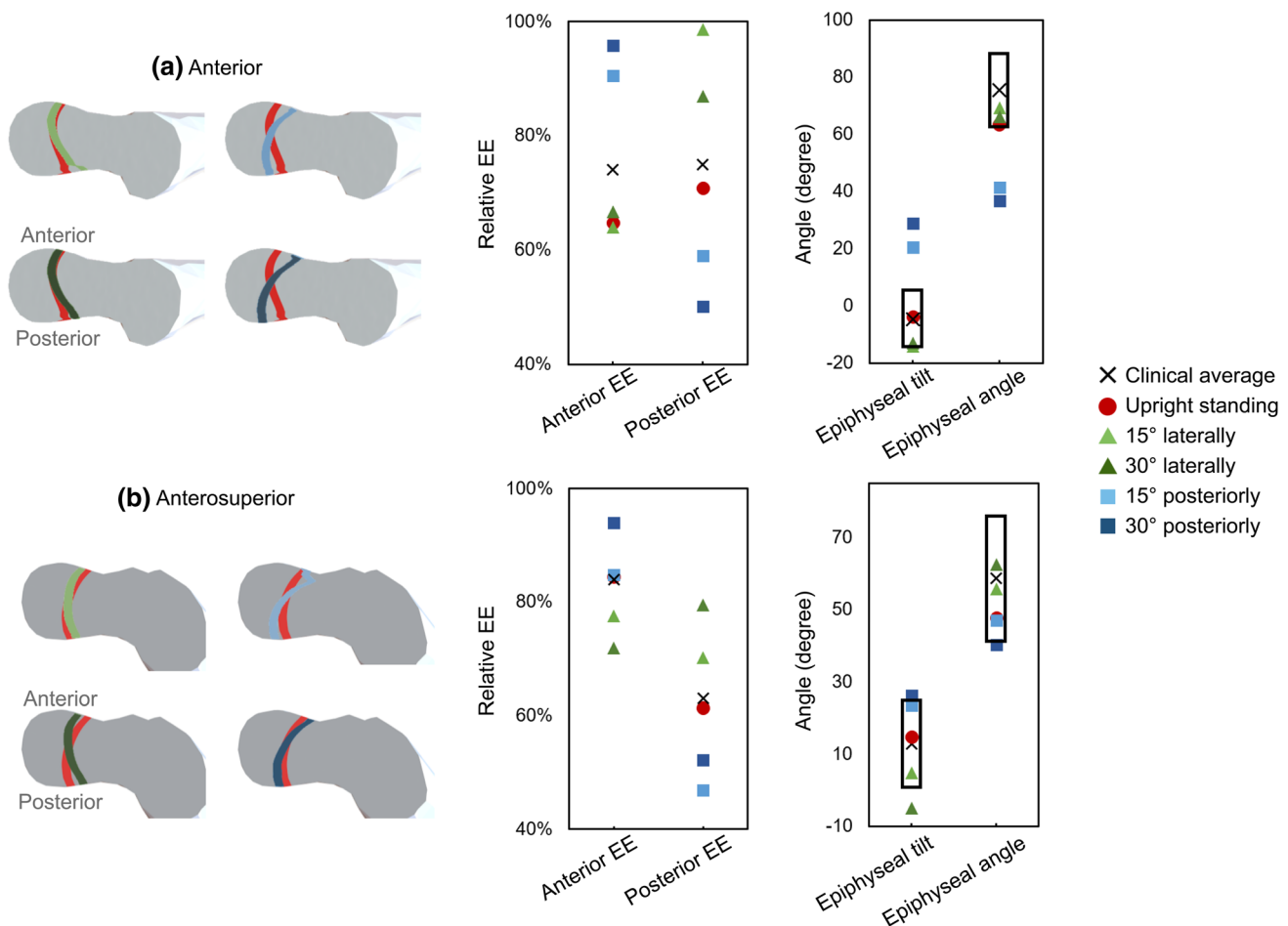


**Fig. 8** Anatomical measurements in the **a** anterior and **b** anterosuperior planes. The boxes on the graph show the normal range of the values from clinical data for epiphyseal tilt and angle (Novais et al. 2018; Siebenrock et al. 2004). Negative values correspond to posterior tilt

these orientations as 3D surfaces and characterized them with the two-dimensional contour plots of the growth plate height with respect to a reference plane perpendicular to the neck axis.

Because shear stress was minimized across the growth plate, not surprisingly octahedral shear stress on the generated growth plates was significantly reduced. Interestingly the hydrostatic stress distribution, though different at the baseline growth plate under the different loading conditions, was similar in the optimized growth plates for all loads so that the maximum of the hydrostatic stress moved to the center of the growth plate for all the cases (Fig. 10). These stress distributions are significant as they have been used to predict growth and ossification patterns (Carter and Wong 1988b, 2003; Piszczatowski 2011; Shefelbine and Carter 2004a, b).

Our novel method for assessing the shape and orientation of the growth plate allowed us to compare the entire three-dimensional surface. Despite of the simplification in our loading condition, the plate of minimum shear stress for

upright standing load oriented similarly to the growth plate of typically developing child. Also, our observation in 3D indicated that the orientation of the growth plates resulting from the hip flexion load was similar to the growth plate in subjects with cam morphology, as the anterosuperior portion moved further from the reference plane tangent to the head.

The parametric study of the hip joint force in laterally and posteriorly directions resulted in the growth plates almost perpendicular to the load. Alterations in the anatomical parameters quantified the influence of the growth plate orientation caused by the change in the joint force direction. The posteriorly directed load significantly shifted the growth plate to an anteriorly tilted position. The laterally directed load resulted in medial tilt of the growth plate. We hypothesized that the growth plate adopts a plane of minimum shear, and our simplified models are similar to clinical measurements of typically developing children. The predictions also suggest that growth plate alterations in cam morphology may be caused by changes in the direction of the joint load, particularly the load experienced when in



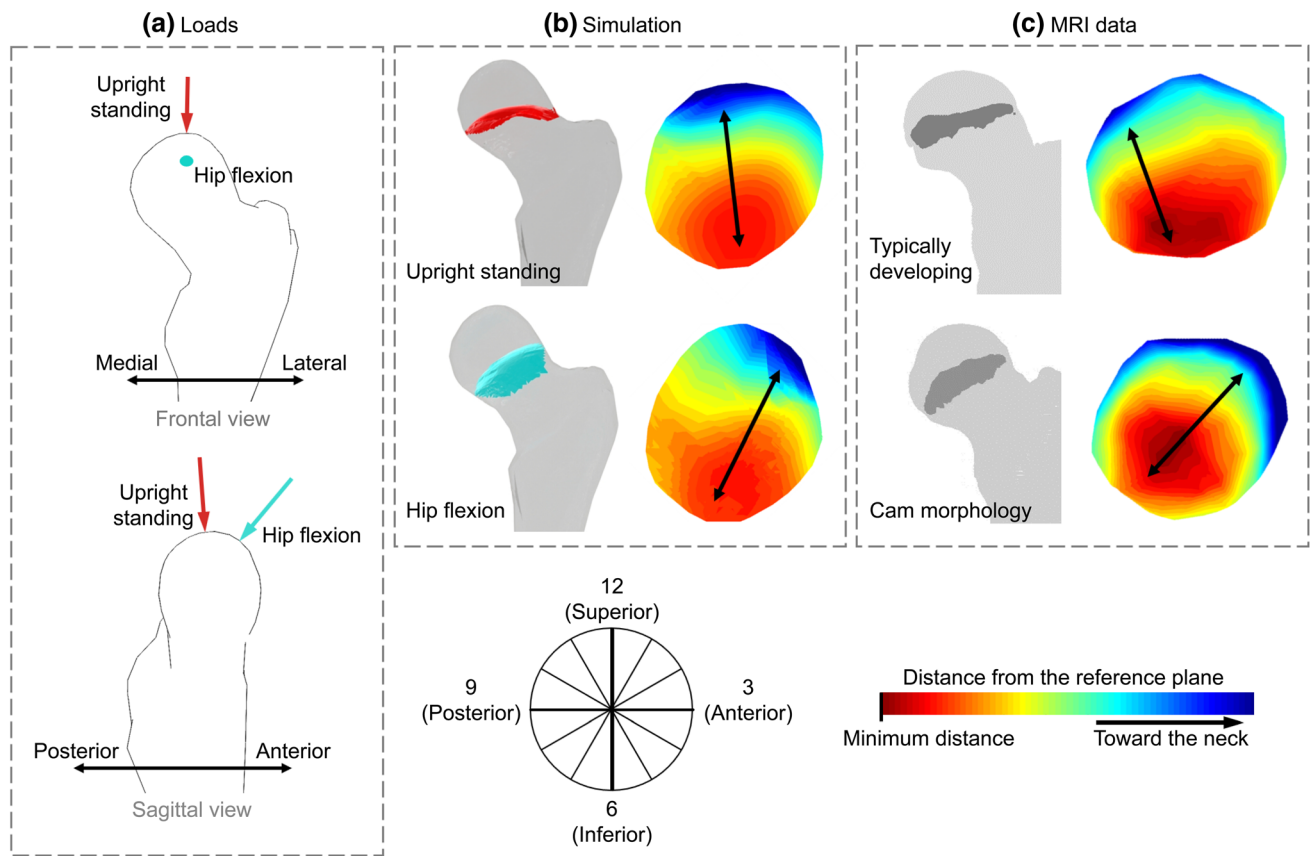


**Fig. 9** Simulated growth plates for upright standing and standing in hip flexion loads. **a** The upright standing and standing in hip flexion loads location. **b** Frontal view of the simulated femoral growth plates and height of the growth plates with respect to the defined reference

plane for upright standing and standing in hip flexion. **c** The 3D shape of the growth plates for a representative typically developing subject and a subject with cam morphology from MRI data. Arrows on the contour plot indicate the growth plate tilt

a position of increased hip flexion. Interestingly previous study on patients with FAI syndrome showed that they have increased hip flexion and anterior pelvic tilt during single leg step-down and walking compared to the control group (Lewis et al. 2018a, b). In this model, we assume that the growth plate adopts an orientation of minimum shear to a single load vector. We used one representative femur of a 7-year-old and parameterized loads. Though the geometry and loading conditions were simplified, the model allowed us to explore the influence of load direction on growth plate orientation. The daily loading on the hip is time-variant in magnitude and direction, and growth plate morphology is likely the result of a weighted average of daily loadings. In future work, combining a patient-specific model with patient-specific gait data and realistic dynamic loading conditions will result in more reliable growth plate predictions. However, presented results illustrate the general trends in growth plate orientation, indicating that altered growth plate shape may provide clues to the causative loading conditions. Additionally, we used isotropic, homogenous, linear elastic material properties though bone and growth plate cartilage

are anisotropic, inhomogeneous, and poro-viscoelastic (Cohen et al. 1998; Radhakrishnan et al. 2004; Sergerie et al. 2009). These common modeling assumptions are used when there is little experimental data to inform more accurate material properties and when the material properties will have a smaller effect on stress directions than loading conditions (Carter and Wong 2003; Shefelbine 2002). We modeled the gradient in mineralization below the growth plate with a transition zone and a linear gradient of modulus. Preliminary sensitivity studies demonstrated that the metaphyseal (distal) transition zone influenced stresses in the growth plate due to the modulus mismatch. In this study, we did not examine how the bone attains this state of minimum shear by modeling the growth of the bone. Future work will examine how stresses on the growth plate may influence growth of the bone into this plane of minimum shear. Future work will also compare predicted growth plate morphologies with clinical data from more subjects with altered hip growth, such as in cerebral palsy, slipped capital femoral epiphysis and femoracetabular impingement.

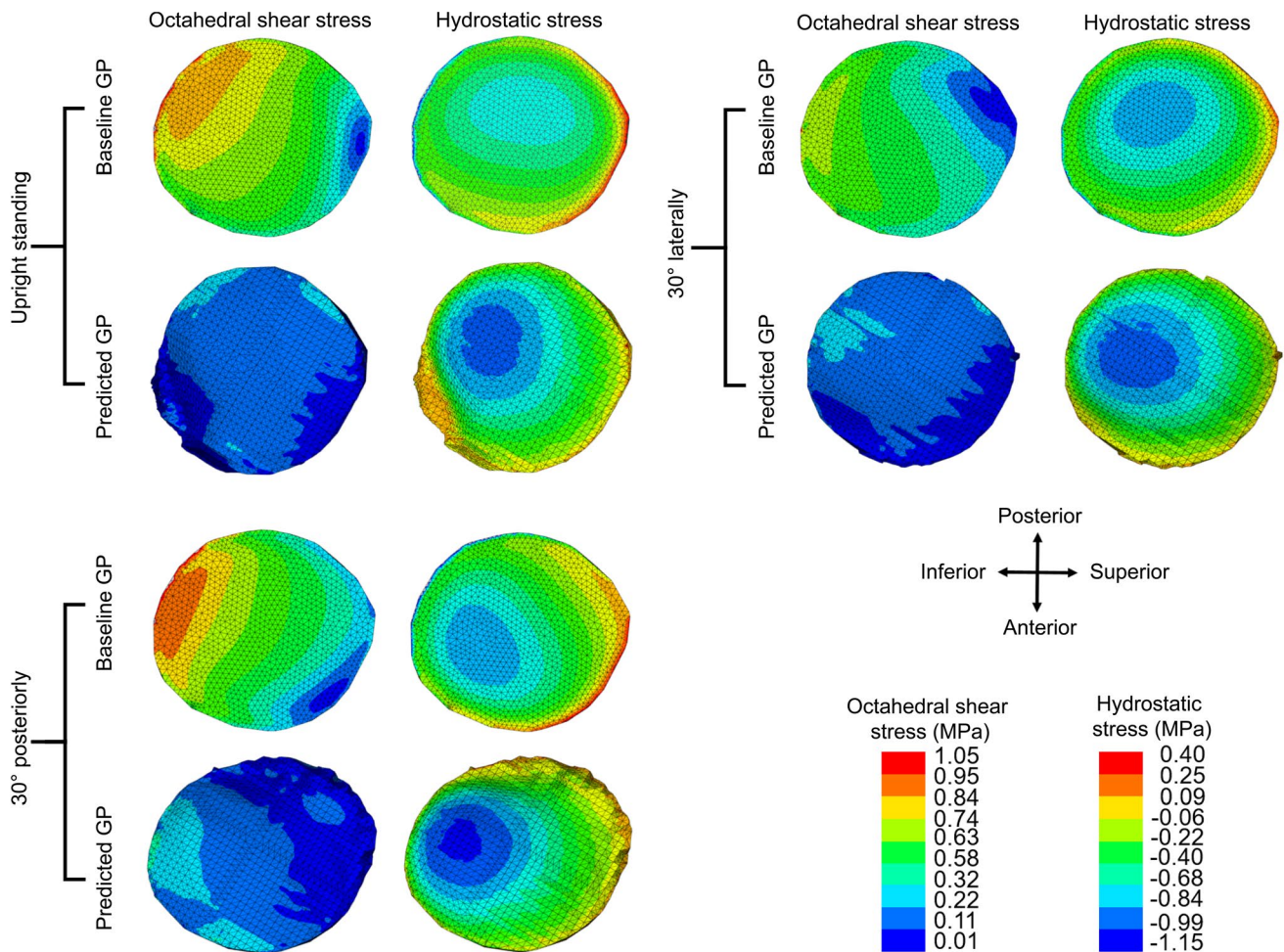


**Fig. 10** Octahedral shear stress and hydrostatic stress over the growth plate in the baseline growth plate versus predicted geometry for upright standing and hip flexion. The shears stress on the predicted growth plate was decreased significantly

In conclusion, this investigation helped us to have a better understanding of the influence of physical activities and particularly hip joint load on the femoral growth plate morphology. The results can be used to predict and prevent developmental bone deformities by identifying positions and movements which result in an anteriorly tilted joint force.

### Compliance with ethical standards

**Conflict of interest** The authors declare that they have no conflict of interest.

### References

- Abad V et al (2002) The role of the resting zone in growth plate chondrogenesis. *Endocrinology* 143:1851–1857
- Agricola R et al (2014) A cam deformity is gradually acquired during skeletal maturation in adolescent and young male soccer

- players: a prospective study with minimum 2-year follow-up. *Am J Sports Med* 42:798–806
- Atkins PR et al (2019) Which two-dimensional radiographic measurements of cam femoroacetabular impingement best describe the three-dimensional shape of the proximal femur? *Clin Orthop Related Res* 477:242–253
- Audenaert EA, Baelde N, Huyse W, Vigneron L, Pattyn C (2011) Development of a three-dimensional detection method of cam deformities in femoroacetabular impingement. *Skelet Radiol* 40:921–927
- Barton C, Salineros MJ, Rakhra KS, Beaulé PE (2011) Validity of the alpha angle measurement on plain radiographs in the evaluation of cam-type femoroacetabular impingement. *Clin Orthop Related Res* 469:464–469
- Bergmann G, Graichen F, Rohlmann A (1993) Hip joint loading during walking and running, measured in two patients. *J Biomech* 26:969–990
- Bergmann G, Deuretzbacher G, Heller M, Graichen F, Rohlmann A, Strauss J, Duda G (2001) Hip contact forces and gait patterns from routine activities. *J Biomech* 34:859–871
- Bergmann G, Bender A, Dymke J, Duda G, Damm P (2016) Standardized loads acting in hip implants. *PLoS one* 11:e0155612

- Carriero A, Jonkers I, Shefelbine SJ (2011) Mechanobiological prediction of proximal femoral deformities in children with cerebral palsy. *Comput Methods Biomech Biomed Eng* 14:253–262
- Carriero A, Zavatsky A, Stebbins J, Theologis T, Lenaerts G, Jonkers I, Shefelbine SJ (2014) Influence of altered gait patterns on the hip joint contact forces. *Comput Methods Biomech Biomed Eng* 17:352–359
- Carter DR, Wong M (1988a) Mechanical stresses and endochondral ossification in the chondroepiphysis. *J Orthop Res* 6:148–154
- Carter DR, Wong M (1988b) The role of mechanical loading histories in the development of diarthrodial joints. *J Orthop Res* 6:804–816
- Carter DR, Wong M (2003) Modelling cartilage mechanobiology. *Philos Trans Royal Soc Lond B Biol Sci* 358:1461–1471
- Castro-Abril HA, Gutiérrez ML, Garzón-Alvarado DA (2016) Proximal femoral growth plate mechanical behavior: comparison between different developmental stages. *Comput Biol Med* 76:192–201
- Chung S, Batterman S, Brighton C (1976) Shear strength of the human femoral capital epiphyseal plate. *J Bone Jt Surg Am* 58:94–103
- Clohisey JC et al (2009) Radiographic evaluation of the hip has limited reliability. *Clin Orthop Relat Res* 467:666–675
- Cohen B, Lai W, Mow V (1998) A transversely isotropic biphasic model for unconfined compression of growth plate and chondroepiphysis. *J Biomech Eng* 120:491–496
- Farzaneh S, Paseta O, Gómez-Benito M (2015) Multi-scale finite element model of growth plate damage during the development of slipped capital femoral epiphysis. *Biomech Model Mechanobiol* 14:371–385
- Ganz R, Parvizi J, Beck M, Leunig M, Nötzli H, Siebenrock KA (2003) Femoroacetabular impingement: a cause for osteoarthritis of the hip. *Clin Orthop Related Res* 417:112–120
- Giorgi M, Carriero A, Shefelbine SJ, Nowlan NC (2015) Effects of normal and abnormal loading conditions on morphogenesis of the prenatal hip joint: application to hip dysplasia. *J Biomech* 48:3390–3397
- Gómez-Benito M, Moreo P, Pérez M, Paseta O, García-Aznar J, Barrios C, Doblaré M (2007) A damage model for the growth plate: application to the prediction of slipped capital epiphysis. *J Biomech* 40:3305–3313
- Harris MD, Datar M, Whitaker RT, Jurrus ER, Peters CL, Anderson AE (2013a) Statistical shape modeling of cam femoroacetabular impingement. *J Orthop Res* 31:1620–1626
- Harris MD, Reese SP, Peters CL, Weiss JA, Anderson AE (2013b) Three-dimensional quantification of femoral head shape in controls and patients with cam-type femoroacetabular impingement. *Ann Biomed Eng* 41:1162–1171
- Johnson AC, Shaman MA, Ryan TG (2012) Femoroacetabular impingement in former high-level youth soccer players. *Am J Sports Med* 40:1342–1346. <https://doi.org/10.1177/0363546512439287>
- Kandzierski G, Matuszewski Ł, Wójcik A (2012) Shape of growth plate of proximal femur in children and its significance in the aetiology of slipped capital femoral epiphysis. *Int Orthop* 36:2513–2520
- Kang RW, Yanke AB, Orias AE, Inoue N, Nho SJ (2013) Emerging ideas: novel 3-D quantification and classification of cam lesions in patients with femoroacetabular impingement. *Clin Orthop Related Res* 471:358–362
- Kienle K-P, Keck J, Werlen S, Kim Y-J, Siebenrock K-A, Mamisch TC (2012) Femoral morphology and epiphyseal growth plate changes of the hip during maturation: MR assessments in a 1-year follow-up on a cross-sectional asymptomatic cohort in the age range of 9–17 years. *Skelet Radiol* 41:1381–1390
- Lewis CL, Khuu A, Loverro KL (2018a) Gait alterations in femoroacetabular impingement syndrome differ by sex. *J Orthop Sports Phys Therapy* 48:649–658
- Lewis CL, Loverro KL, Khuu A (2018b) Kinematic differences during single-leg step-down between individuals with femoroacetabular impingement syndrome and individuals without hip pain. *J Orthop Sports Phys Ther* 48:270–279
- Monazzam S, Bomar JD, Pennock AT (2013) Idiopathic cam morphology is not caused by subclinical slipped capital femoral epiphysis: an MRI and CT study. *Orthop J Sports Med* 1:2325967113512467
- Novais E, Kienle K-P, Miller P, Bowen G, Kim Y-J, Bixby S (2018) Age- and gender-specific variations of the epiphyseal tilt and epiphyseal angle in adolescents without hip pathology. *J Children's Orthop* 12:152–159
- Palmer A et al (2018) Physical activity during adolescence and the development of cam morphology: a cross-sectional cohort study of 210 individuals. *Br J Sports Med* 52:601–610. <https://doi.org/10.1136/bjsports-2017-097626>
- Piszczatowski S (2011) Material aspects of growth plate modelling using Carter's and Stokes's approaches. *Acta Bioeng Biomech* 13:3–14
- Poussa M, Schlenzka D, Yrjönen T (2003) Body mass index and slipped capital femoral epiphysis. *J Pediatric Orthop B* 12:369–371
- Radhakrishnan P, Lewis NT, Mao JJ (2004) Zone-specific micromechanical properties of the extracellular matrices of growth plate cartilage. *Ann Biomed Eng* 32:284–291
- Sankar WN, Nevitt M, Parvizi J, Felson DT, Leunig M (2013) Femoroacetabular impingement: defining the condition and its role in the pathophysiology of osteoarthritis. *JAAOS J Am Acad Orthop Surg* 21:S7–S15
- Sergerie K, Lacoursière M-O, Lévesque M, Villemure I (2009) Mechanical properties of the porcine growth plate and its three zones from unconfined compression tests. *J Biomech* 42:510–516
- Shapiro F (2002) *Pediatric orthopedic deformities*. Elsevier, Amsterdam
- Shefelbine SJ (2002) *Mechanical regulation of bone growth fronts and growth plates*. Stanford University, Stanford
- Shefelbine SJ, Carter DR (2004a) Mechanobiological predictions of femoral anteversion in cerebral palsy. *Ann Biomed Eng* 32:297–305
- Shefelbine SJ, Carter DR (2004b) Mechanobiological predictions of growth front morphology in developmental hip dysplasia. *J Orthop Res* 22:346–352
- Siebenrock K, Wahab KA, Werlen S, Kalhor M, Leunig M, Ganz R (2004) Abnormal extension of the femoral head epiphysis as a cause of cam impingement. *Clin Orthop Related Res* 418:54–60
- Siebenrock K-A, Ferner F, Noble P, Santore R, Werlen S, Mamisch TC (2011) The cam-type deformity of the proximal femur arises in childhood in response to vigorous sporting activity. *Clin Orthop Related Res* 469:3229
- Siebenrock KA, Behning A, Mamisch TC, Schwab JM (2013a) Growth plate alteration precedes cam-type deformity in elite basketball players. *Clin Orthop Related Res* 471:1084–1091
- Siebenrock KA, Kaschka I, Frauchiger L, Werlen S, Schwab JM (2013b) Prevalence of cam-type deformity and hip pain in elite ice hockey players before and after the end of growth. *Am J Sports Med* 41:2308–2313
- Smith J (1962) The relationship of epiphyseal plates to stress in some bones of the lower limb. *J Anat* 96:58
- Villemure I, Stokes IA (2009) Growth plate mechanics and mechanobiology. A survey of present understanding. *J Biomech* 42:1793–1803

- Yadav P, Shefelbine SJ, Gutierrez-Farewik EM (2016) Effect of growth plate geometry and growth direction on prediction of proximal femoral morphology. *J Biomech* 49:1613–1619
- Yadav P, Shefelbine SJ, Pontén E, Gutierrez-Farewik EM (2017) Influence of muscle groups' activation on proximal femoral growth tendency. *Biomech Model Mechanobiol* 16:1869–1883
- Zupanc O, Križancic M, Daniel M, Mavcic B, Antolic V, Igljic A, Kralj-Igljic V (2008) Shear stress in epiphyseal growth plate is a risk factor for slipped capital femoral epiphysis. *J Pediatric Orthop* 28:444–451
- Publisher's Note** Springer Nature remains neutral with regard to jurisdictional claims in published maps and institutional affiliations.